Magn Reson Mater Phy (2012) 25:127–133
DOI 10.1007/s10334-011-0286-3

RESEARCH ARTICLE

Optimization of background suppression for arterial spin labeling perfusion imaging

Nasim Maleki · Weiying Dai · David C. Alsop

Received: 7 June 2011 / Revised: 29 August 2011 / Accepted: 22 September 2011 / Published online: 19 October 2011

Abstract
Object To present an algorithm for optimization of background suppression pulse timing for arterial spin labeling (ASL) perfusion imaging.
Materials and methods An algorithm for optimization of background suppression pulse timing is proposed. Numerical optimization of timing of the background suppression pulses is investigated in both constrained and unconstrained ASL sequences. The performance of the parameters from the algorithm is evaluated in phantom and also in vivo in five human subjects.
Results The background signal is suppressed to less than 1% across a broad range of T1s with a modest number of inversion pulses using the timings acquired from the numerical optimization algorithm proposed in this study. The performance of the parameters from the algorithm is also confirmed in vivo.
Conclusion Successful background suppression over a broad range of tissues is achievable. Values for optimal pulse timing in both pulsed and continuous ASL studies are reported to facilitate sequence design with different labeling parameters.

N. Maleki (✉)
Department of Radiology, Children's Hospital Boston,
300 Longwood Ave, Boston, MA 02115, USA
e-mail: nasim.maleki@childrens.harvard.edu

N. Maleki
Department of Radiology, Harvard Medical School,
Boston, MA, USA

W. Dai · D. C. Alsop
Department of Radiology, Beth Israel Deaconess Medical Center
and Harvard Medical School, Boston, MA, USA

Keywords Magnetic resonance imaging · Arterial spin labeling · Perfusion · Background suppression

Introduction

Arterial spin labeling (ASL) offers means of investigating tissue perfusion in numerous functional and pathological states non-invasively. Though the ASL perfusion signal is small, improved array receive coils and higher field strength acquisition have made sensitive measurement of the signal possible. The measured perfusion signal is on the order of few percent relative to the static background tissue, and motion artifacts in clinical studies of difficult patient populations can reduce the effective sensitivity of ASL despite these hardware improvements.

Several investigators have emphasized the advantages of background suppression in continuous [1] and pulsed [2] ASL sequences using multiple inversion pulses to further improve ASL sensitivity. Dixon et al. first proposed the idea of multiple inversion recovery (MIR) suppression to reduce static background signal in a subtractive inflow technique for short delay, angiographic sequences [3]. The application of multiple inversion pulses following a saturation pulse could be timed to null several tissues with different T_1s, as compared to nulling the signal from a tissue with a single T_1 with application of single inversion. Mani et al. extended the MIR concept for ASL angiography and took into account the effect of variations in the B_1 and B_0 fields on the background suppression over a range of T_1 [4].

Because of the longer labeling times and lower signal intensities in ASL perfusion studies, as compared to ASL angiography, the degree of background suppression becomes more critical. The optimization of background suppression for perfusion studies has previously relied on

nulling T1s of several normal tissues or on algorithms not described or characterized in detail. In this study we describe an algorithm to optimize the timing of background suppression pulses to decrease the background static signal for a broad range of T_1s. This algorithm is applicable to both pulsed ASL (PASL) and continuous ASL (CASL) studies of any chosen timing of labeling.

Materials and methods

Background suppression schemes

All considered background suppression approaches first apply a spatially selective saturation, followed by one or more inversion pulses prior to imaging, Fig. 1. Numerical optimization of background suppression was performed for two basic schemes. One of the schemes employed a constraint that no inversions could occur during a specified time interval (constrained scheme). This constraint can be used to allow an uninterrupted window for continuous labeling of a desired labeling duration and post-labeling delay to be applied. The other scheme had no such constraint (unconstrained scheme). Both of the schemes did have a weaker constraint on the spacing between pulses to allow for finite pulse duration of 20 ms.

The unconstrained background suppression can be combined with a PASL experiment by adding a labeling pulse immediately either before or after the saturation, Fig. 1a. Alternatively, inversion labeling outside the imaged region can be performed at any time during the sequence. However, for time efficiency, there is little advantage to label long after the saturation pulse. For PASL, all background suppression inversion pulses after the labeling pulse must be non-selective. If any inversion pulses are applied before the labeling pulse, they should be selective.

CASL can, in principle, be performed with either background suppression scheme. The constrained background suppression can be used to fit the labeling duration, with the desired post-labeling delay, between background suppression pulses, Fig. 1b. As for PASL, background suppression inversion pulses must be selective before labeling. Pulses after labeling can be either selective or non-selective, but are indicated as non-selective in the figure because non-selective pulses after labeling were employed in our experiments.

CASL and unconstrained background suppression can also be performed [5] with background suppression pulses occurring during the labeling duration i.e. interleaved labeling with background suppression, Fig. 1c. Each time an inversion is applied, the label must be switched to control and vice versa. All inversion pulses applied before and during labeling must be selective. With interleaved labeling and background suppression, each inversion pulse will cause some additional loss of efficiency due to the imperfect sharpness of the inversion pulse and the labeling plane itself that may depend upon the vascular geometry and velocity. Further experiments may be required to

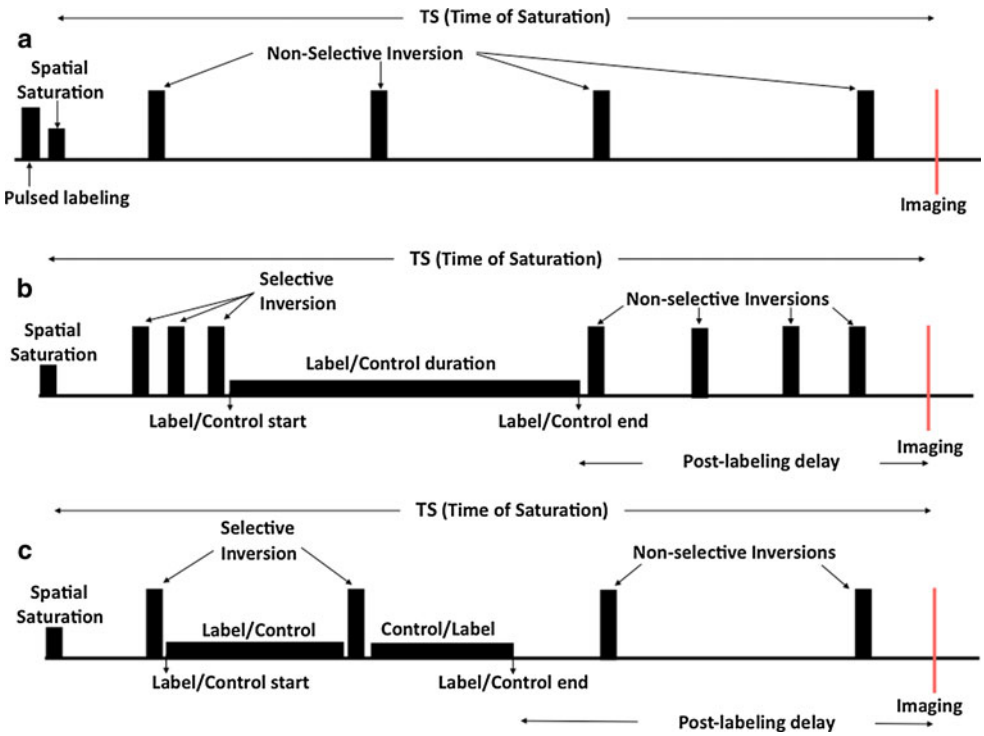

Fig. 1 The timing diagram for the background suppression. **a** Unconstrained scheme, **b** constrained scheme and **c** also an unconstrained background suppression scheme interleaved with CASL. The 'pulsed labeling' pulse in (**a**) could be any desired pulse that is applied during label or control of any PASL technique. In the FAIR technique, for instance, this would be a non-selective inversion (180°) for label and a selective inversion (180°) for control. TS is the time saturation of which is the time between the saturation pulse and the time of image acquisition

investigate the tradeoff between the flexibility of unconstrained background suppression and any efficiency loss from the interleaved labeling.

Optimization algorithm

The background suppression timing was optimized by casting it as a nonlinear optimization problem with bounds on the pulse timings in MATLAB (MathWorks Inc., Natick, MA). The squared residual background signal summed across a target range of T_1s, with optional weights, was minimized using an iterative minimization technique based on an implementation of Shor's r-algorithm [6]. In the results reported here, residual background signal for T_1s ranging from 250 to 4,200 ms, in steps of 1 ms, were equally weighted in the optimization. The optimization of background suppression timing was investigated in both constrained and unconstrained schemes. For various number of pulses (up to 9 non-selective pulses in unconstrained schemes and up to four selective pulses pre-labeling and up to 8 non-selective pulses post-labeling in constrained schemes) the optimum timing of the pulses that minimized the total squared residual background signal was found. The optimum number of pulses was then determined to be the minimum number of pulses that would yield residual background signal below 1% for for T_1s ranging from 250 to 4,200 ms for all the desired post-labeling delays.

For constrained schemes, the optimization was solved for two different time of saturation (TS) values. TS is the time separation (between saturation pulse and the time of imaging (TS = 3,000 ms or 6,000 ms). These two values were selected to have optimum solutions for both a shorter TR sequence (TS = 3,000 ms) and a longer TR sequence (TS = 6,000 ms). Each TS imposes an upper limit on the sum of the post labeling delay and labeling duration. A range of post-labeling delays from 250 to 2,500 ms in steps of 250 ms were considered with labeling durations from 250 ms to TS minus the post-labeling delay.

Inefficiency of the inversion pulses (3.2-ms hyperbolic tangent pulses, 0.18 G B_1) was included in the magnetization equation in the form of a coefficient, χ, and was modeled based on fitting a polynomial to the experimentally measured results reported in [7]. Including fixed high efficiencies for short T_1 fat and long T_1 fluid, the efficiencies were modeled as:

$$\chi = \begin{cases} -0.998 & 250 < T_1 < 449 \\ (-2.245e-15)T_1^4 + (2.378e-11)T_1^3 - (8.987e-8)T_1^2 + (1.442e-4)T_1 + (9.1555e-1) & 450 < T_1 < 2000 \\ -0.998 & 2001 < T_1 < 4200 \end{cases}$$

The longitudinal magnetization, M_z, a time TS after the saturation and n inversions will then be described by the following equation:

$$M_z = 1 + (M_z(0) - 1)\chi e^{-\mathrm{TS}/T_1} + \sum_{m=1}^{n} (\chi^m - \chi^{m-1}) e^{-t_m/T_1}$$

where, $M_z(0)$ is the initial magnetization and t_m is the spacing between pulse m and TS (inversions are counted from TS).

For the unconstrained optimization, analytical equations were derived for calculation of the timing of the background suppression pulses at any desired inversion time by fitting the results to a 2nd degree polynomial in Ts. The expansion coefficients were determined by least squares fitting. This optimization is valid for both PASL and unconstrained CASL. For PASL, Ts should typically be nearly identical with the inversion time (TI) of labeling since the labeling pulse would be applied either immediately before or after the saturation pulses. For the constrained optimization for CASL, tables of timing of the pulses were generated instead.

Imaging studies

Studies were performed on a 3.0 Tesla GE HD MR system with an 8-channel array head coil on five healthy subjects and on a phantom consisting of an array of tubes containing MnCl-doped deionized water in various concentrations [8] for validation. Human studies followed a protocol approved by the local institutional review board and all subjects gave written informed consent after explanation of the nature and possible consequences of the study.

The optimal constrained background suppression scheme determined by simulation was combined with pulsed-CASL [9] and single slice axial brain images at the level of the optic nerve heads were acquired. Images were acquired using a 2D half Fourier single shot fast spin echo SSFSE sequence. Imaging parameters for pulsed-CASL were FOV = 24 cm, Matrix = 96 × 96, TR = 7,000 ms, TE = 36.5 ms (min TE), bandwidth = 20.83 kHz, and slice thickness = 10 mm, TS = 6,000 ms. The labeling slab was also in the axial plane, approximately 5 cm below the slice. Selective 500 μs long Hanning shaped RF pulses with 1,500 μs spacing were applied at equal spacing during both label and control sequences [10]. A gradient

amplitude of 0.6 G, an average B1 of 20 mG, and an average gradient of 0.15 G were employed for the labeling [10].

Suppression of signal was achieved by first selectively saturating the imaging region. The saturation pulses begin the background suppression series of pulses. Four quadratic phase saturation pulses [11] were played with the last centered at 6,000 ms prior to imaging (pulses were 10 ms in duration, 12.5 kHz in bandwidth, and played 17 ms apart). Crusher-gradient pulses of incrementally increasing magnitude between the RF pulses were used to prevent refocusing of transverse magnetization. Selective "C-shape" frequency offset corrected inversion (FOCI) pulses [12], with durations 15.36 ms and bandwidth 1.08 kHz ($\beta = 509\ s^{-1}$ and $\mu = 6.2$) were used for the three inversion pulses prior to labeling. After labeling, a series of nonselective adiabatic hyperbolic-secant inversion pulses [13] of 10 ms duration and 1.4 kHz bandwidth ($\beta = 970\ s^{-1}$ and $\mu = 4.5$) were applied. Though these pulses differed from the tanh pulses assumed in the simulations, the efficiencies of optimal hyperbolic secant based pulses are very similar [7].

Image pairs (label and control) were acquired at delays of 0.5, 0.75, 1, 1.25, 1.5, and 2.5 s. The labeling duration for these post-labeling delays were 0.5, 0.75, 1, 1.25, 1.5, and 2 s, respectively. The pairs were repeated 20 times to improve signal-to-noise ratio by averaging. At the end, two images were acquired with all the labeling and background suppression pulses turned off. Similar imaging with two averages was performed on phantoms.

All brain image data were saved as raw echo intensities and transferred to a Linux workstation. Images for each coil of the 8-channel phased array coil were reconstructed offline with custom tools developed in the IDL programming environment (ITT Visual Information Systems, Boulder CO). The data for each coil was averaged for all the repetitions and the resulting average was phase corrected. Close to optimal combination of the complex coil image data was achieved by sum of individual coil images weighted and phased by the coil sensitivity ratios derived from smoothing the non background suppressed image by a 9×9 Gaussian filter [14]. This method decreased the bias due to the rectification of negative noise contributions in the reconstructed perfusion images.

All phantom images were saved and transferred in DICOM format to a Linux workstation and analyzed using tools provided in ImageJ (http://rsbweb.nih.gov/ij/index.html). Similar circular ROIs (984.38 mm^3) were defined on the tubes and the mean signal intensity was measured.

Results

Simulations

The algorithm was able to determine optimal pulse timings for all saturation times and labeling timings considered. In general, the background suppression performance improved with the number of inversion pulses employed but such good suppression is achieved with 3–5 pulses that benefit from additional pulses is minimal. The optimal number of pulses for unconstrained schemes was found to be four pulses for all the TSs. The optimum number of pulses for unconstrained pulses is valid for both the unconstrained CASL sequence and PASL sequence and Table 1 can be used to determine the timing of the inversion pulses for any given TS. The optimal number of pulses in constrained CASL sequence was found to be three selective inversion pulses applied prior to labeling and four non-selective inversion pulses applied post-labeling for all post labeling delays.

The constraint in timing imposed for uninterrupted CASL generally degraded background suppression relative to the unconstrained optimization. In fact constrained background suppression less than 1% could not be achieved for labeling durations longer than the post-labeling delay. This degradation tended to occur as the duration of the gap between pulses, the labeling time, increased beyond the time from the end of the gap to imaging, i.e. the post-labeling delay. This suggests that background suppression of CASL experiments with long duration of labeling and short post-labeling delay will benefit from applying inversion pulses during the labeling.

Table 1 Coefficients of the quadratic polynomial equations that can be used to derive the optimal timing of the inversion pulses for PASL sequence

Coefficients	Pulse 1	Pulse 2	Pulse 3	Pulse 4
P1	−1.385e−005	−4.649e−005	−6.983e−005	−4.308e−005
P2	0.08497	0.3216	0.648	0.9219
P3	−7.52	−21.42	−28.95	−19.4

Linear model f(TS)* = p1*TS^2 + p2*TS + p3 Coefficients (with 95% confidence bounds. In case of PASL, TS is typically equal to the inversion time, TI, of labeling. In the case of unconstrained CASL, TS must be greater than or equal to the post-labeling delay plus the labeling duration

Table 2 Optimal timing of the pulses for post-labeling delays ranging from 250 ms to 2,500 ms for CASL sequence

TS	Delay (ms)	Labeling (ms)	Non-selective post labeling inversion pulses (ms)				Selective pre-labeling inversion pulses (ms)			Saturation pulse (ms)
3,000	250	250	42.08	100.09	120.1	230	520	951.39	1413.37	1630.61
	500	500	95.26	299.14	349.04	479.89	1,020	1,818	2,622	2,979.69
	750	750	20	85.36	276.68	730	1,520	2,468.57	2,960	2,980
	1,000	1,000	20.02	111.47	375.7	980	2,020.17	2,753.38	2,773.42	2,793.54
	1,250	1,250	20	91.91	374.83	1,230	2,520	2,940	2,960	2,980
	1,500	1,000	20.01	173.35	615.64	1,480	2,520	2,540.02	2,560.02	2,980
6,000	250	250	39.25	88.3	109.4	229.92	535.78	1,008.98	1,538.48	1,795.31
	500	500	94.22	295.01	346.63	479.96	1,020.02	1,833.51	2,685.63	3,080.44
	750	750	20	91.5	287.77	729.99	1,520	2,580.79	3,216.66	3,243.09
	1,000	1,000	20	125.19	405.8	980	2,020	3,615.09	5,288.7	5,979.99
	1,250	1,250	20.01	151.49	511.45	1,229.59	2,520	4,463.43	5,815.02	5,835.27
	1,500	1,500	20.01	170.62	600.83	1,480	3,020	4,969.21	5,959.88	5,980
	2,000	2,000	107.47	459.47	1,169.87	2,480	4,520	5,939.98	5,959.98	5,980
	2,500	2,000	106.94	457.55	1,166.52	2,477.2	4,520.38	5,938.16	5,958.19	5,979.75

The optimal timings are derived for TS = 3,000 ms and 6,000 ms (refer to "Results" section)

* It is assumed that image is acquired at time 0 and timing of the pulses is measured in reference to the image acquisition time

For the unconstrained optimization, the optimal inversion times were readily fit to polynomial functions of the TS. The fit parameters are tabulated in Table 1. For the constrained optimization, polynomial fits were less successful and particular values are reported for interesting labeling times. The optimal timing for unconstrained background suppression with such long labeling duration CASL sequences can be derived from Table 2 by selecting a TS greater than the post-labeling delay plus the labeling duration (Table 2).

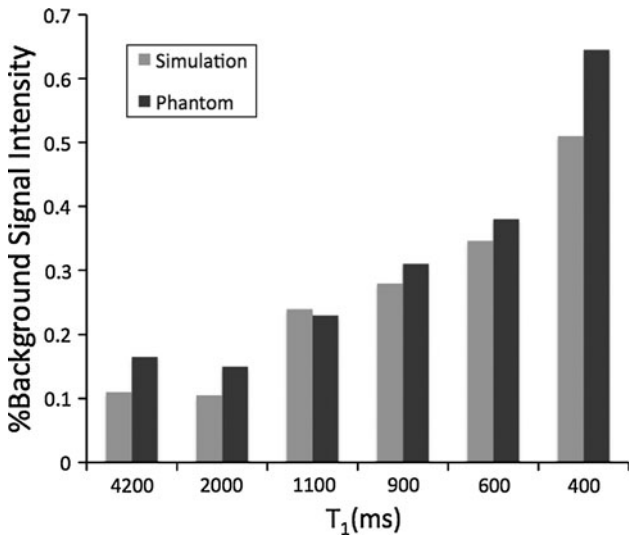

Fig. 2 Simulated and experimental (Background suppressed PCASL, TS = 6,000) background intensity for background suppressed MnCl-doped phantoms at post labeling delay of 1 s

Experimental measurements

Similar trends in the level of background intensity against T_1 were seen in simulated and phantom results both qualitatively and quantitatively. In Fig. 2 the simulations results are shown against imaging results obtained with background suppressed pulsed-CASL sequence from MnCl-doped phantoms at post labeling delay of 1,000 ms (TS = 6,000 ms). T_1 and T_2 values of these phantoms were previously measured using inversion recovery and multiple spin-echo acquisitions [8]. The magnitude of the residual signal relative to the background signal intensity, for various T_1s confirmed the validity of the optimization resulting from our simulations.

Single slice background suppressed control images and corresponding PCASL perfusion images acquired at post labeling delays of 750, 1,250, and 2,500 ms (labeling durations of 750, 1,250, and 2,000 ms correspondingly) are shown in a subject in Fig. 3. MR images were of similar quality in all subjects. Motion between the acquisitions of images at various delays was not an important problem in any of the subjects. The group average percentage of the static background signal remaining in gray matter, fat and vitreous following background suppression is shown in Fig. 4. The level of background suppression is a function of the post labeling delay (in CASL) or inversion time (in PASL), labeling duration (in CASL) and the tissue. As an example of the effectiveness of the proposed optimized background suppression successful background suppression facilitated imaging of retinal perfusion [15] as it can be seen in the perfusion images of Fig. 3. The presence of

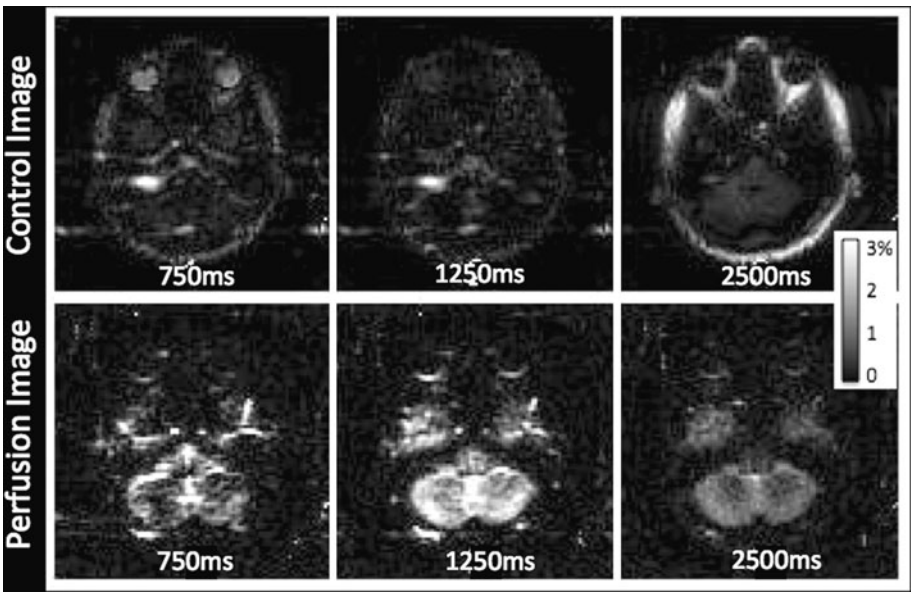

Fig. 3 Single slice background suppressed control image (*upper row*) and corresponding perfusion images (*lower row*) at 0.75 s (1), 1.25 s (2), and 2.5 s (3) obtained with constrained background suppressed pulsed-continuous ASL technique. Images are on the same scale relative to unsuppressed signal. The *grayscale* represents the percentage signal relative to unsuppressed background

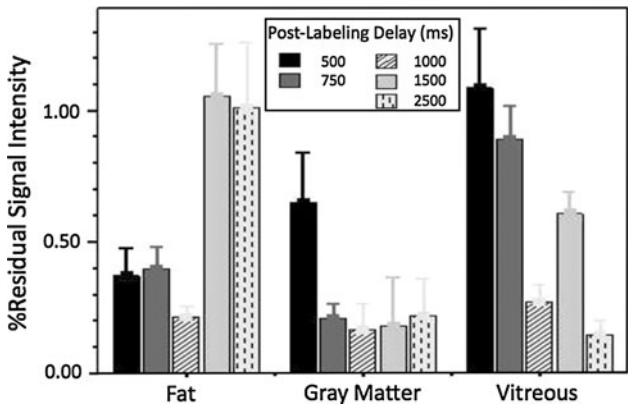

Fig. 4 Percentage of the residual static background signal remaining in the in vivo images following background suppression. Three categories of T_1 values are shown corresponding to fat, *gray* matter and vitreous (of importance for retinal blood flow imaging). The residual background signal is reported for post labeling delays of 500–2,500 ms

eye motion and a large background signal intensity gradient between the vitreous and the periorbital fat which can give rise to excessive noise when small motions and thus using an effective background suppression approach would be even more important in imaging such structures.

Discussion

In our study almost 100-fold decreases in background signal intensity to the noise level have been achieved such that the ASL signal change exceeded the residual signal from static tissue. Our results were validated both in vivo and in phantoms. It has previously been reported that the use of background suppression reduces the standard deviation of the ASL signal measurement that indicates greater sensitivity for ASL on a pixel-by-pixel basis as compared to unsuppressed ASL images [7]. With the help of background suppression, the application of susceptibility insensitive, spin echo based imaging sequences has been realized in multi-shot volumetric acquisitions, and more recently, with the incorporation of parallel imaging, single-shot acquisition of the whole brain has been achieved [16–18].

Our optimization strategy differed form earlier approaches, such as that of Mani et al. [4], that selected particular T1s for exact nulling. Instead, we employed a least squares minimization strategy across a range of T1s typical in tissue. This least squares approach is particularly helpful in maintaining background suppression quality in the presence of pathology, which can alter T1s from the expected values in normal tissue. Use of a priori weights for particular T1s, though not explicitly used in our optimizations, can be used to emphasize particular tissue T1s, such as gray and white matter. However, the high level of background suppression, achieved with uniform weighting suggests such a priori weighting may not be necessary for most applications.

The aim of this study was to provide tools for designing an effective background suppression scheme for any ASL technique. Using Tables 1 and 2 one can derive the timing of the optimal pulses for any desired PASL or interrupted CASL labeling. This flexibility is not available for uninterrupted CASL (constrained scheme) for which optimal timing for specific post labeling delays are reported only. However the range and number of these post-labeling delays covers the entire ASL signal time curve with a

reasonable temporal resolution. Also shorter labeling durations could be employed for all of post labeling durations reported without affecting the quality of background suppression. It should also be noted that with the constrained scheme, the labeling duration is limited, otherwise a reduction of background suppression effectiveness occurs.

Our acquisition has been single slice, primarily because the study of retinal perfusion was a potentially challenging one and we began exploration with an anatomically focused sequence. The optimization methods can readily be applied to 3D acquisitions and have been used in recent paper with whole brain volumetric imaging [5]. Multi-slice 2D imaging poses additional challenges for background suppression since there is no single imaging time [19]. Optimization for 2D sequences may benefit from these methods but additional timing and efficiency considerations must be added.

Conclusion

Suppression of the background signal to less than 1% across a broad range of T_1s is readily achievable with a modest number of inversion pulses. Values for optimal pulse timing in both pulsed and continuous ASL studies are reported in this paper to facilitate sequence design with different labeling parameters. One of the potential applications of the optimal background suppression schemes proposed in this paper could be to a class of ASL methods in which perfusion-weighted images are obtained without a control acquisition. The low level of residual static background signal achieved here does emphasize the possibility of ASL measurement without subtraction [20, 21] either for resting perfusion or motion insensitive activation related changes.

Acknowledgments This work was supported in part by a grant from the National Institutes of Health through grant MH80729.

References

1. Alsop D, Detre J (1999) Background suppressed 3D RARE ASL perfusion imaging. In: International society for magnetic resonance in medicine 7th scientific meeting, Philadelphia, p 601
2. Ye FQ, Frank JA, Weinberger DR, McLaughlin AC (2000) Noise reduction in 3D perfusion imaging by attenuating the static signal in arterial spin tagging (ASSIST). Magn Reson Med 44(1):92–100
3. Dixon WT, Sardashti M, Castillo M, Stomp GP (1991) Multiple inversion recovery reduces static tissue signal in angiograms. Magn Reson Med 18(2):257–268
4. Mani S, Pauly J, Conolly S, Meyer C, Nishimura D (1997) Background suppression with multiple inversion recovery nulling: applications to projective angiography. Magn Reson Med 37(6):898–905
5. Dai W, Robson PM, Shankaranarayanan A, Alsop DC (2011) Reduced resolution transit delay prescan for quantitative continuous arterial spin labeling perfusion imaging. Magn Reson Med (in press)
6. Shor NZ (1985) Minimization methods for non-differentiable functions. Springer, New York
7. Garcia DM, Duhamel G, Alsop DC (2005) Efficiency of inversion pulses for background suppressed arterial spin labeling. Magn Reson Med 54(2):366–372
8. de Bazelaire CM, Duhamel GD, Rofsky NM, Alsop DC (2004) MR imaging relaxation times of abdominal and pelvic tissues measured in vivo at 3.0 T: preliminary results. Radiology 230(3):652–659
9. Dai W, Garcia D, de Bazelaire C, Alsop DC (2008) Continuous flow-driven inversion for arterial spin labeling using pulsed radio frequency and gradient fields. Magn Reson Med 60(6):1488–1497
10. Garcia DM, de Bazelaire C, Alsop DC (2005) Pseudo-continuous flow driven adiabatic inversion for arterial spin labeling. in: international society for magnetic resonance in medicine 13th scientific meeting, Miami, Florida, USA, p 9
11. Kunz D (1987) Frequency-modulated radiofrequency pulses in spin-echo and stimulated-echo experiments. Magn Reson Med 4(2):129–136
12. Ordidge RJ, Wylezinska M, Hugg JW, Butterworth E, Franconi F (1996) Frequency offset corrected inversion (FOCI) pulses for use in localized spectroscopy. Magn Reson Med 36(4):562–566
13. O'Dell LA, Harris KJ, Schurko RW (2010) Optimized excitation pulses for the acquisition of static NMR powder patterns from half-integer quadrupolar nuclei. J Magn Reson 203(1):156–166
14. Bydder M, Larkman DJ, Hajnal JV (2002) Combination of signals from array coils using image-based estimation of coil sensitivity profiles. Magn Reson Med 47(3):539–548
15. Maleki N, Dai W, Alsop DC (2011) Blood flow quantification of the human retina with MRI. NMR Biomed 24(1):104–111
16. Duhamel G, Alsop D (2004) Single-shot susceptibility insensitive whole brain 3D perfusion imaging with ASL. In: International society for magnetic resonance in medicine 12th scientific meeting, Kyoto, Japan, p 518
17. Fernandez-Seara MA, Wang Z, Wang J, Rao HY, Guenther M, Feinberg DA, Detre JA (2005) Continuous arterial spin labeling perfusion measurements using single shot 3D GRASE at 3 T. Magn Reson Med 54(5):1241–1247
18. Gunther M, Oshio K, Feinberg DA (2005) Single-shot 3D imaging techniques improve arterial spin labeling perfusion measurements. Magn Reson Med 54(2):491–498
19. St Lawrence KS, Frank JA, Bandettini PA, Ye FQ (2005) Noise reduction in multi-slice arterial spin tagging imaging. Magn Reson Med 53(3):735–738
20. Blamire AM, Styles P (2000) Spin echo entrapped perfusion image (SEEPAGE). A nonsubtraction method for direct imaging of perfusion. Magn Reson Med 43(5):701–704
21. Duyn JH, Tan CX, van Gelderen P, Yongbi MN (2001) High-sensitivity single-shot perfusion-weighted fMRI. Magn Reson Med 46(1):88–94